Shape Analysis of C-B-splines

Rongjun Wu
Department of Applied Mathematics, Northwestern Polytechnical University, Xi'an, PR China
Email: wrj2140@163.com

Guohua Peng
Department of Applied Mathematics, Northwestern Polytechnical University, Xi'an, PR China
Email: penggh@nwpu.edu.cn

***Abstract*—The shape features of planar C-B-spline segments are analyzed. The necessary and sufficient conditions are derived for the curve having one or two inflection points, a loop or a cusp, or be locally or globally convex. All conditions are completely characterized by the relative position of the control polygon's side vectors, and are summarized in three kinds of shape diagrams in terms of the linear independence of the three side vectors. Moreover, it is proved that a spatial C-B-spline segment has no singularities and generalized inflection points.**

***Index Terms*—C-B-spline, Singularity, Inflection point, Convexity, Shape diagram**

I. INTRODUCTION

The C-B-spline segments introduced in [1, 2] not only inherit many geometric properties from B-splines, but also have an adjustable shape parameter, and can represent arcs of circles and ellipse, as well as some transcend curves such as cycloid and helix precisely. In [3], the authors proved that C-B-spline segments are generated by a normalized totally positive basis, and constructed a normalized basis of C-B-splines which admits optimal shape preserving and stability properties.

It is well known that the distributions of singular points and inflection points, and the (local or global) convexity of parametric curves play very important roles in designing curves. For instance, in numerically controlled milling operations, many of algorithms rely on the fact that the trace of the curve is smooth-an assumption that is violated if a cusp is present. Inflection points often indicate unwanted oscillations in applications such as automobile body design and aerodynamics, and surface that has a cross-section curve possessing a loop cannot be manufactured.

This topic (also known as shape classification or geometric characterization of a curve in computer aided geometric design) has been studied before from different points of view [4–18]. For the case of general parametric curves the reader can see [4, 5]. For planar cubic parametric curves some useful results can be found in [6–11]. For the rational case one can refer to [12–14]. For C-curves a classical shape diagram (similar to those in [6, 7]) was obtained in [15]. However in the papers [4–15], the difference between global and local convexity was untouched. In [16] a necessary and sufficient condition for global convexity of planar curves was presented. In [17], the authors did not only investigate inflection points and singularities but also the global and local convexity of the planar cubic trigonometric Bézier curves with a shape parameter. A different class of shape diagram of B-spline curves with shape parameters was discussed in [18]. Some applications research related to this topic can be found in [19-21].

In this paper we apply the method presented in [11], which is based on the theory of envelope and topological mapping, to C-B-spline segment, we obtain the distribution regions of singular points and inflection points without much difficulty. According to the linear independence of three side vectors, we obtain three kinds of shape diagrams, which are different from that in [17], for the planar C-B-spline segment. Two of the three kinds of shape diagrams are different from that in [18]. Furthermore we discussed the influence of shape parameter on the shape diagram. In addition, we show that the spatial C-B-spline segment is a twisted curve.

The rest of this paper is organized as follows. In Section 2, we introduce the construction of the C-B-spline segments. In Section 3, the cusps, inflection points, loops and convexity of the planar C-B-spline segment are discussed. In Section 4, the influence of shape parameter on the shape diagram is illustrated. In Section 5, we deal with the spatial C-B-spline segment. We close in Section 6 with a brief summary of our work.

II. C-B-SPLINE SEGMENTS

The C-B-spline segment introduced in [1, 2] can be defined in the following way:

Definition 1: Let $\boldsymbol{d}_i\,(i=0,1,2,3)$ be given control points and α be a real value with $0<\alpha<\pi$. The curve

$$\boldsymbol{r}(t)=\sum_{i=0}^{3}\boldsymbol{d}_i b_i(t),\quad t\in[0,1], \tag{1}$$

is called C-B-spline segment with a parameter α, where

doi:10.4304/jcp.9.3.750-757

$$\begin{cases} b_0(t) = [\alpha - \alpha t - \sin(\alpha - \alpha t)]/[2\alpha(1-\cos\alpha)], \\ b_3(t) = b_0(1-t), \\ b_1(t) = b_3(t) - 2b_0(t) + 1 - t, \\ b_2(t) = b_1(1-t). \end{cases} \quad (2)$$

It was proved that curves which are piecewise C-B-spline segments are continuously differentiable up to order two and the limit of $\boldsymbol{r}(t)$ approaches a uniform B-spline curve as α tends to zero in [1], more details can refer to [2]. It is not difficult to see that the curve is actually a straight line segment if all four control points are collinear but coincident, and collapses to a single point if all four control points are coincident. In the following section we discuss the shape features of planar C-B-spline segments. Without loss of generality, we suppose that the control points $\boldsymbol{d}_i (i = 0,1,2,3)$ are not collinear and are denoted by two dimensional column vectors in Sections 3 and 4.

III. Shape Analysis of Planar C-B-spline Segments

We recall the following preliminary knowledge before discussion. The interested reader is referred to [4, 10, 11, 16, 22] for further details.

Definition 2**:** If the tangent vector $\boldsymbol{r}'(t)$ of the parametric curve $\boldsymbol{r}(t)$ changes direction oppositely at t_0, then the curve $\boldsymbol{r}(t)$ has a cusp at t_0 (see [4, 11]).

Definition 3**:** Let $\gamma(t) = \boldsymbol{r}'(t) \times \boldsymbol{r}''(t)$, where given two vectors $\boldsymbol{x} = (x_1, x_2)^{\mathrm{T}}$ and $\boldsymbol{y} = (y_1, y_2)^{\mathrm{T}}$, we define the cross product $\boldsymbol{x} \times \boldsymbol{y} = x_1 y_2 - x_2 y_1$. If $\gamma(t)$ changes sign at t_0 with $\boldsymbol{r}'(t_0) \neq 0$, then the curve $\boldsymbol{r}(t)$ has an inflection point at t_0 (see [4, 10, 11]).

Definition 4: If there exists $t_1 \neq t_2$ such that $\boldsymbol{r}(t_1) = \boldsymbol{r}(t_2)$, then the curve $\boldsymbol{r}(t)$ has a loop (see [11]).

Definition 5: Let

$$\gamma(t) = \boldsymbol{r}'(t) \times \boldsymbol{r}''(t),$$
$$m(t) = \boldsymbol{r}'(0) \times [\boldsymbol{r}(t) - \boldsymbol{r}(0)],$$
$$n(t) = [\boldsymbol{r}(t) - \boldsymbol{r}(0)] \times \boldsymbol{r}'(t),$$

And suppose that the curve $\boldsymbol{r}(t)$ ($t \in [0,1]$) has no singularities (cusps or loops). If none of $\gamma(t)$, $m(t)$ and $n(t)$ changes sign for all $t \in [0,1]$, then the curve r(t) is globally convex. If $\gamma(t)$ does not change sign for all $t \in [0,1]$, but there exists $t_0 \in (0,1)$ such that $m(t)$ or $n(t)$ changes sign at t_0, then the curve $\boldsymbol{r}(t)$ is locally convex (see [16]).

Definition 6: For given family of curves C_t: $F(x, y, t) = 0$ with a single parameter t, C: $f(x, y) = 0$ is called as the envelop curve of the given family of curves C_t, if the curve C satisfies that every point on C belongs to one curve in the given family C_t and C tangents to C_t at the point. The equation of C can be determined by solving the simultaneous equations

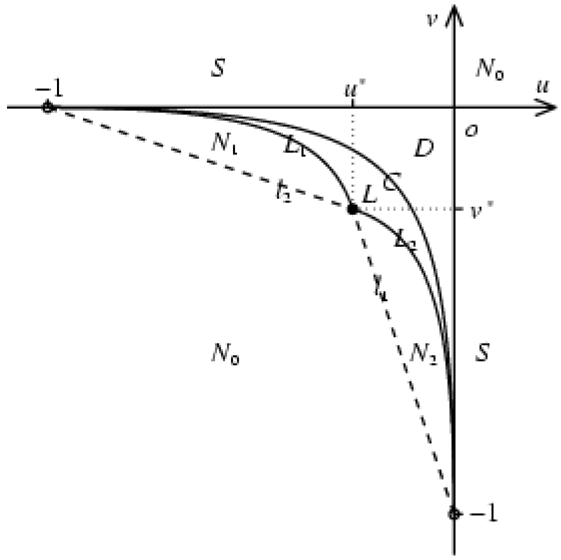

Figure 1. Shape diagram of planar C-B-spline segment with $\boldsymbol{a}_1 \times \boldsymbol{a}_3 \neq 0$.

$$\begin{cases} F(x, y, t) = 0, \\ F_t'(x, y, t) = 0, \end{cases}$$

with respect to x and y (see [22]).

Let $\boldsymbol{a}_i = \boldsymbol{d}_i - \boldsymbol{d}_{i-1} (i = 1,2,3)$, the curve (1) can be rewritten as

$$\boldsymbol{r}(t) = \boldsymbol{d}_0 + [1 - b_0(t)]\boldsymbol{a}_1 + [b_2(t) + b_3(t)]\boldsymbol{a}_2 + b_3(t)\boldsymbol{a}_3. \quad (3)$$

First, we suppose that the side vectors $\boldsymbol{a}_1$ and $\boldsymbol{a}_3$ are linearly independent; in other words $\boldsymbol{a}_1 \times \boldsymbol{a}_3 \neq 0$. Then the side vector $\boldsymbol{a}_2$ can be expressed as linear combination of the two side vectors $\boldsymbol{a}_1$ and $\boldsymbol{a}_3$; that is $\boldsymbol{a}_2 = u\boldsymbol{a}_1 + v\boldsymbol{a}_3$, where $(u, v) = (\boldsymbol{a}_2 \times \boldsymbol{a}_3, \boldsymbol{a}_1 \times \boldsymbol{a}_2)/(\boldsymbol{a}_1 \times \boldsymbol{a}_3)$. The coefficients u and v clearly indicate the relative position of the control polygon's side vectors. Substituting $\boldsymbol{a}_2 = u\boldsymbol{a}_1 + v\boldsymbol{a}_3$ into (3), we have

$$\begin{aligned} \boldsymbol{r}(t) = \boldsymbol{d}_0 &+ \{1 - b_0(t) + u[b_2(t) + b_3(t)]\}\boldsymbol{a}_1 \\ &+ \{b_3(t) + v[b_2(t) + b_3(t)]\}\boldsymbol{a}_3. \end{aligned} \quad (4)$$

The following theorem shows the relation between the position of point (u, v) in uv-plane and the shape features of the curve segment (4).

Theorem 1**:** Assume that $\boldsymbol{a}_2 = u\boldsymbol{a}_1 + v\boldsymbol{a}_3$ with $\boldsymbol{a}_1 \times \boldsymbol{a}_3 \neq 0$. Then, the shape features of the curve segment (4) are completely determined by the position of point (u, v) in uv-plane (see Fig. 1) as follows:

- if $(u, v) \in N_0$, then $\boldsymbol{r}(t)$ is globally convex and has no inflection points and singularities;
- if $(u, v) \in N_1 \cup N_2$, then $\boldsymbol{r}(t)$ is locally convex and has no inflection points and singularities;
- if $(u, v) \in S$, then $\boldsymbol{r}(t)$ has a single inflection point and no singularities;
- if $(u, v) \in D$, then $\boldsymbol{r}(t)$ has two inflection points and no singularities;
- if $(u, v) \in C$, then $\boldsymbol{r}(t)$ has a cusp and no loops and inflection points;

- if $(u,v)\in L$, then $\boldsymbol{r}(t)$ has a loop and no cusps and inflection points.

The regions mentioned above are defined as:
$S=\{(u,v)\,|\,uv<0\}\bigcup\{(u,0)\,|\,-1<u<0\}\bigcup\{(0,v)\,|\,-1<v<0\}$;
D is the open region that is bounded by the coordinate axis and the curve C;
L is the region that is bounded by curves C, L_1 and L_2, and $L_1\subset L$, $L_2\subset L$, but $C\not\subset L$;
N_1 is the region that is bounded by curves L_1 and l_2, and $l_2\not\subset N_1$;
N_2 is the region that is bounded by curves L_2 and l_1, and $l_1\not\subset N_2$;
N_0 is the complement of the union $C\bigcup S\bigcup D\bigcup L\bigcup N_1\bigcup N_2$ in uv-plane;
where the parametric equations of the curves C, L_i and l_i are defined as:

$$C:\begin{cases} u=\dfrac{\cos(\alpha-\alpha t)-1}{\cos(\alpha t)+\cos(\alpha-\alpha t)-2\cos\alpha}, \\ v=\dfrac{\cos(\alpha t)-1}{\cos(\alpha t)+\cos(\alpha-\alpha t)-2\cos\alpha}, \end{cases} \quad 0<t<1, \tag{5}$$

$$L_1:\begin{cases} u=\dfrac{\sin\alpha-\alpha t-\sin(\alpha-\alpha t)}{\sin\alpha+\sin(\alpha t)-\sin(\alpha-\alpha t)-2\alpha t\cos\alpha}, \\ v=\dfrac{-\alpha t+\sin(\alpha t)}{\sin\alpha+\sin(\alpha t)-\sin(\alpha-\alpha t)-2\alpha t\cos\alpha}, \end{cases} \quad 0<t\le 1, \tag{6}$$

$$L_2:\begin{cases} u=\dfrac{-\alpha+\alpha t+\sin(\alpha-\alpha t)}{\sin\alpha+\sin(\alpha-\alpha t)-\sin(\alpha t)-2(\alpha-\alpha t)\cos\alpha}, \\ v=\dfrac{\sin(\alpha)-\alpha+\alpha t-\sin(\alpha t)}{\sin\alpha+\sin(\alpha-\alpha t)-\sin(\alpha t)-2(\alpha-\alpha t)\cos\alpha}, \end{cases} \quad 0\le t<1, \tag{7}$$

$$l_1:\begin{cases} u=(1-t)u^*, \\ v=-t+(1-t)v^*, \end{cases} \quad 0\le t\le 1, \tag{8}$$

$$l_2:\begin{cases} u=-t+(1-t)u^*, \\ v=(1-t)v^*, \end{cases} \quad 0\le t\le 1, \tag{9}$$

and $u^*=v^*=-\dfrac{(\alpha-\sin\alpha)}{2(\sin\alpha-\alpha\cos\alpha)}$.

Proof:

The proof is composed of four parts corresponding to the case of cusps, inflection points, loops and convexity, respectively.

A. The Case of Cusps

According to Definition 2, the necessary condition that the curve $\boldsymbol{r}(t)$ has cups is $\boldsymbol{r}'(t)=0$. From (4), we have

$$\{-b_0'(t)+u[b_2'(t)+b_3'(t)]\}\boldsymbol{a}_1+\{b_3'(t)+v[b_2'(t)+b_3'(t)]\}\boldsymbol{a}_3=0.$$

By the linear independence of $\boldsymbol{a}_1$ and $\boldsymbol{a}_3$, we obtain

$$\begin{cases} u=b_0'(t)/[b_2'(t)+b_3'(t)], \\ v=-b_3'(t)/[b_2'(t)+b_3'(t)]. \end{cases} \tag{10}$$

Substituting (2) into (10), we get (5), that is the parametric equations of the curve C.

Conversely, suppose that the point (u_0,v_0) lies on the curve C and $u_0=u(t_0)$, $v_0=v(t_0)$, where $t_0\in(0,1)$, then $\boldsymbol{r}''(t_0)\neq 0$. Otherwise, from $\boldsymbol{r}''(t_0)=0$, we can get

$$\begin{cases} u_0=b_0''(t_0)/[b_2''(t_0)+b_3''(t_0)], \\ v_0=-b_3''(t_0)/[b_2''(t_0)+b_3''(t_0)]. \end{cases}$$

It follows that $u_0+v_0=1$, which contradicts $(u_0,v_0)\in C$. Therefore, according to the Taylor expansion

$$\boldsymbol{r}'(t)=\boldsymbol{r}''(t_0)(t-t_0)+o(t-t_0),$$

we know that $\boldsymbol{r}'(t)$ changes direction oppositely at t_0.

Hence we have proved that the curve segment (4) has a cusp if and only if $(u,v)\in C$.

B. The Case of Inflection Points

By direct computation from (4), we can get

$$\gamma(t)=\boldsymbol{r}'(t)\times\boldsymbol{r}''(t)=f(t;u,v)\boldsymbol{a}_1\times\boldsymbol{a}_3,$$

where

$$f(t;u,v)=-\begin{vmatrix} b_0'(t) & b_3'(t) \\ b_0''(t) & b_3''(t)\end{vmatrix}+u\begin{vmatrix} b_2'(t) & b_3'(t) \\ b_2''(t) & b_3''(t)\end{vmatrix}+v\begin{vmatrix} b_0'(t) & b_1'(t) \\ b_0''(t) & b_1''(t)\end{vmatrix}.$$

According to Definition 3, the point $\boldsymbol{r}(t_0)$ is an inflection point if and only if $f(t;u,v)$ changes sign at t_0. In the uv-plane, the possible region of inflection points must be covered by the family of straight lines $f(t;u,v)=0$. After solving the simultaneous equations

$$\begin{cases} f(t;u,v)=0, \\ f_t'(t;u,v)=0, \end{cases}$$

with respect to u and v, we get (10).

From Definition 6 we know that the curve C is just the envelope of the family of straight lines $f(t;u,v)=0$. The curve C is strictly convex continuous curve, so that the region swept by the tangent lines of the curve C is $S\bigcup D$ (see Fig. 1), i.e. the possible region that results in inflection points.

Apparently, the curve C has at least a tangent line $f(t_0;u,v)=0$ passing through an arbitrary point (u_0,v_0) located in $S\bigcup D$. Note that $f_t'(t_0;u_0,v_0)\neq 0$ (otherwise, it contradicts $(u_0,v_0)\in C$) when $(u_0,v_0)\in S\bigcup D$. Therefore, from the Taylor expansion

$$f(t;u_0,v_0)=f_t'(t_0;u_0,v_0)(t-t_0)+o(t-t_0),$$

we know that $f(t;u_0,v_0)$ changes sign at $t=t_0$, consequently, the point $\boldsymbol{r}(t_0)$ is an inflection point.

Furthermore, when $(u_0,v_0)\in S$, the curve $\boldsymbol{r}(t)$ has a single inflection point because there exists a unique tangent line of the curve C passing through the point (u_0,v_0); when $(u_0,v_0)\in D$, the curve $\boldsymbol{r}(t)$ has two inflection points due to two tangent lines of the curve C passing through the point (u_0,v_0) (see Fig. 1).

C. The Case of Loops

From Definition 4, the sufficient and necessary condition that the curve segment (4) has a loop is that there exists $0 \le t_1 < t_2 \le 1$ such that $\boldsymbol{r}(t_1) - \boldsymbol{r}(t_2) = 0$. It is equivalent to u, v, t_1 and t_2 satisfy the system of equations:

$$\begin{cases} u = \dfrac{b_0(t_2) - b_0(t_1)}{b_2(t_2) + b_3(t_2) - b_2(t_1) - b_3(t_1)}, \\ v = \dfrac{b_3(t_1) - b_3(t_2)}{b_2(t_2) + b_3(t_2) - b_2(t_1) - b_3(t_1)}, \end{cases} (t_1, t_2) \in \Delta, \tag{11}$$

where $\Delta = \{(t_1, t_2) \in \mathbb{R}^2 \mid 0 \le t_1 < t_2 \le 1\}$. The map F: $\Delta \to F(\Delta)$ defined as (11) is a topological mapping. Therefore, the image $L = F(\Delta)$ is a simply connected region in uv-plane, its three boundary curves C, L_1 and L_2 correspond to the three boundary segments of Δ: $t_1 = t_2$, $t_1 = 0$ and $t_2 = 1$, respectively. It follows that the curve C does not belong to the region L while the curves L_1 and L_2 belong to, and the parametric equations of L_1 and L_2 are determined by (6) and (7), respectively.

Thus, we have proved that the curve segment (4) has a loop if and only if $(u, v) \in L$.

Both the curves L_1 and L_2 are monotonically decreasing and strictly convex continuous curves. the curve L_1 intersects the curve L_2 at the point (u^*, v^*), where $u^* = v^* = -(\alpha - \sin\alpha)/[2(\sin\alpha - \alpha\cos\alpha)]$. It can be easily checked that the curve L_1 is tangent to u-axis at $(-1, 0)$ when t tends to 0, and the curve L_2 is tangent to v-axis at $(0, -1)$ when t tends to 1.

D. The Case of Convexity

It is clear that the curve segment (4) has none of inflection points and singular points if the point (u, v) lies in complementary region $N = \mathbb{R}^2 \setminus (C \cup S \cup D \cup L)$. As is shown in Fig. 1, the region N can be divided into N_0, N_1 and N_2, where the region N_1 is bounded by the curve L_1 and the line segment l_2 determined by the two points $(-1, 0)$ and (u^*, v^*), the region N_2 is bounded by the curve L_2 and the line segment l_1 determined by the two points $(0, -1)$ and (u^*, v^*). The line segment $l_i (i = 1, 2)$ is the tangent line of the curve $L_i (i = 1, 2)$ at the point (u^*, v^*).

To distinguish a local convex curve from a global one, as mentioned in Definition 5, we need to consider $\gamma(t)$, $m(t)$ and $n(t)$. By direct computation from (4), we have $m(t) = \varphi(t; u, v)\boldsymbol{a}_1 \times \boldsymbol{a}_3$ and $n(t) = \psi(t; u, v)\boldsymbol{a}_1 \times \boldsymbol{a}_3$, where

$$\varphi(t; u, v) = b_2'(0)\{(1+u)b_3(t) + v[1 - 2b_2(0) - b_1(t)]\}, \tag{12}$$

$$\psi(t; u, v) = \begin{vmatrix} b_2(0) - b_0(t) & b_3(t) \\ -b_0'(t) & b_3'(t) \end{vmatrix} + u \begin{vmatrix} b_2(t) + b_3(t) - b_2(0) & b_3(t) \\ b_2'(t) + b_3'(t) & b_3'(t) \end{vmatrix} + v \begin{vmatrix} b_2(0) - b_0(t) & b_2(t) + b_3(t) - b_2(0) \\ -b_0'(t) & b_2'(t) + b_3'(t) \end{vmatrix}. \tag{13}$$

The equation (12) determines a family of straight lines, which always pass through $(-1, 0)$ in uv-plane, and the slop coefficient of these lines is $k = b_3(t)/[b_1(t) + 2b_2(0) - 1]$. It can be deduced that $v^*/(1+u^*) < k < 0$ holds for $0 < t < 1$, so the region determined by $\varphi(t; u, v) = 0$ with $(u, v) \in N$ is N_1. Therefore $\varphi(t; u_0, v_0)$ changes sign at t_0 when $(u_0, v_0) \in N_1$. In fact, the region N_1 is just the part of the region N, which covered by the tangent lines of the curve L_2 (see Fig.1).

Parametric Equations (6) can be obtained by solving the simultaneous equations

$$\begin{cases} \psi(t; u, v) = 0, \\ \psi_t'(t; u, v) = 0, \end{cases}$$

for the unknown parameters u and v. This implies that the region N_2 is covered by the tangent lines of the curve L_1. If the point (u_0, v_0) lies in the region N_2, then the curve L_1 has a tangent line $\psi(t_0; u, v) = 0$ passing through it, and $\psi_t'(t_0; u_0, v_0) \ne 0$ holds. Thus, according to the Taylor expansion $\psi(t; u_0, v_0) = \psi_t'(t_0; u_0, v_0)(t - t_0) + o(t - t_0)$, we know that $\psi(t; u_0, v_0)$ changes sign at t_0.

In summary, $\gamma(t)$, $m(t)$ and $n(t)$ do not change sign for all $t \in (0,1)$ when $(u_0, v_0) \in N_0 \cup N_1 \cup N_2$, while there exits $t_0 \in (0,1)$ such that $m(t)$ (or $n(t)$) changes sign at t_0 when $(u_0, v_0) \in N_1$ (or N_2).

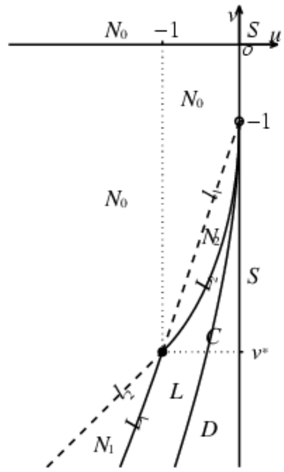

Figure 2: Shape diagram of planar C-B-spline segment with $\boldsymbol{a}_1 \times \boldsymbol{a}_2 \ne 0$.

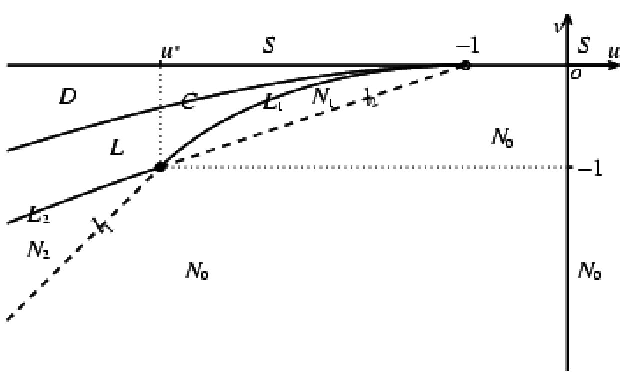

Figure 3: Shape diagram of planar C-B-spline segment with $\boldsymbol{a}_2 \times \boldsymbol{a}_3 \ne 0$.

It follows that the curve segment (4) is globally (or locally) convex if and only if $(u,v)\in N_0$ (or $N_1\bigcup N_2$).

The proof is finished.

Finally, excluding the four control points are collinear, there exist still two cases: (A) $\boldsymbol{a}_1\times\boldsymbol{a}_2\neq 0$, ($B$) $\boldsymbol{a}_2\times\boldsymbol{a}_3\neq 0$.

If $\boldsymbol{a}_1\times\boldsymbol{a}_2\neq 0$, then $\boldsymbol{a}_3=u\boldsymbol{a}_1+v\boldsymbol{a}_2$, where $(u,v)=(\boldsymbol{a}_3\times\boldsymbol{a}_2, \boldsymbol{a}_1\times\boldsymbol{a}_3)/(\boldsymbol{a}_1\times\boldsymbol{a}_2)$, so the curve (3) can be rewritten as:

$$\boldsymbol{r}(t)=\boldsymbol{d}_0+[1-b_0(t)+ub_3(t)]\boldsymbol{a}_1+[b_2(t)+b_3(t)+vb_3(t)]\boldsymbol{a}_2. \quad (14)$$

If $\boldsymbol{a}_2\times\boldsymbol{a}_3\neq 0$, then $\boldsymbol{a}_1=u\boldsymbol{a}_2+v\boldsymbol{a}_3$, where $(u,v)=(\boldsymbol{a}_1\times\boldsymbol{a}_3, \boldsymbol{a}_2\times\boldsymbol{a}_1)/(\boldsymbol{a}_2\times\boldsymbol{a}_3)$, so the curve (3) can be rewritten as:

$$\begin{aligned}\boldsymbol{r}(t)=\boldsymbol{d}_0&+\{b_2(t)+b_3(t)+u[1-b_0(t)]\}\boldsymbol{a}_2\\&+\{b_3(t)+v[1-b_0(t)]\}\boldsymbol{a}_3.\end{aligned} \quad (15)$$

The shape features of the curve segment (14) and (15) are analogous to those of curve segment (4), the associated shape diagrams are shown in Fig. 2 and Fig. 3 respectively.

In case (A) the parametric equations of the curves C, L_i and l_i are determined by:

$$C:\begin{cases}u=\dfrac{\cos(\alpha-\alpha t)-1}{1-\cos(\alpha t)},\\ v=\dfrac{2\cos\alpha-\cos(\alpha t)-\cos(\alpha-\alpha t)}{1-\cos(\alpha t)},\end{cases}\quad 0<t<1, \quad (16)$$

$$L_1:\begin{cases}u=\dfrac{\sin\alpha-\alpha t-\sin(\alpha-\alpha t)}{\alpha t-\sin(\alpha t)},\\ v=\dfrac{2\alpha t\cos\alpha-\sin(\alpha t)+\sin(\alpha-\alpha t)-\sin\alpha}{\alpha t-\sin(\alpha t)},\end{cases}\quad 0<t\leq 1, \quad (17)$$

$$L_2:\begin{cases}u=\dfrac{\alpha-\alpha t-\sin(\alpha-\alpha t)}{\sin\alpha-\sin(\alpha t)-\alpha+\alpha t},\\ v=\dfrac{\sin\alpha-2(\alpha-\alpha t)\cos\alpha+\sin(\alpha-\alpha t)-\sin(\alpha t)}{\sin\alpha-\sin(\alpha t)-\alpha+\alpha t},\end{cases}\quad 0\leq t<1, \quad (18)$$

$$l_1: v+(1+v^*)u+1=0, -1\leq u<0, \quad (19)$$

$$l_2: v-u-(1+v^*)=0, -\infty<u\leq -1, \quad (20)$$

where $v^*=-2(\sin\alpha-\alpha\cos\alpha)/(\alpha-\sin\alpha)$.

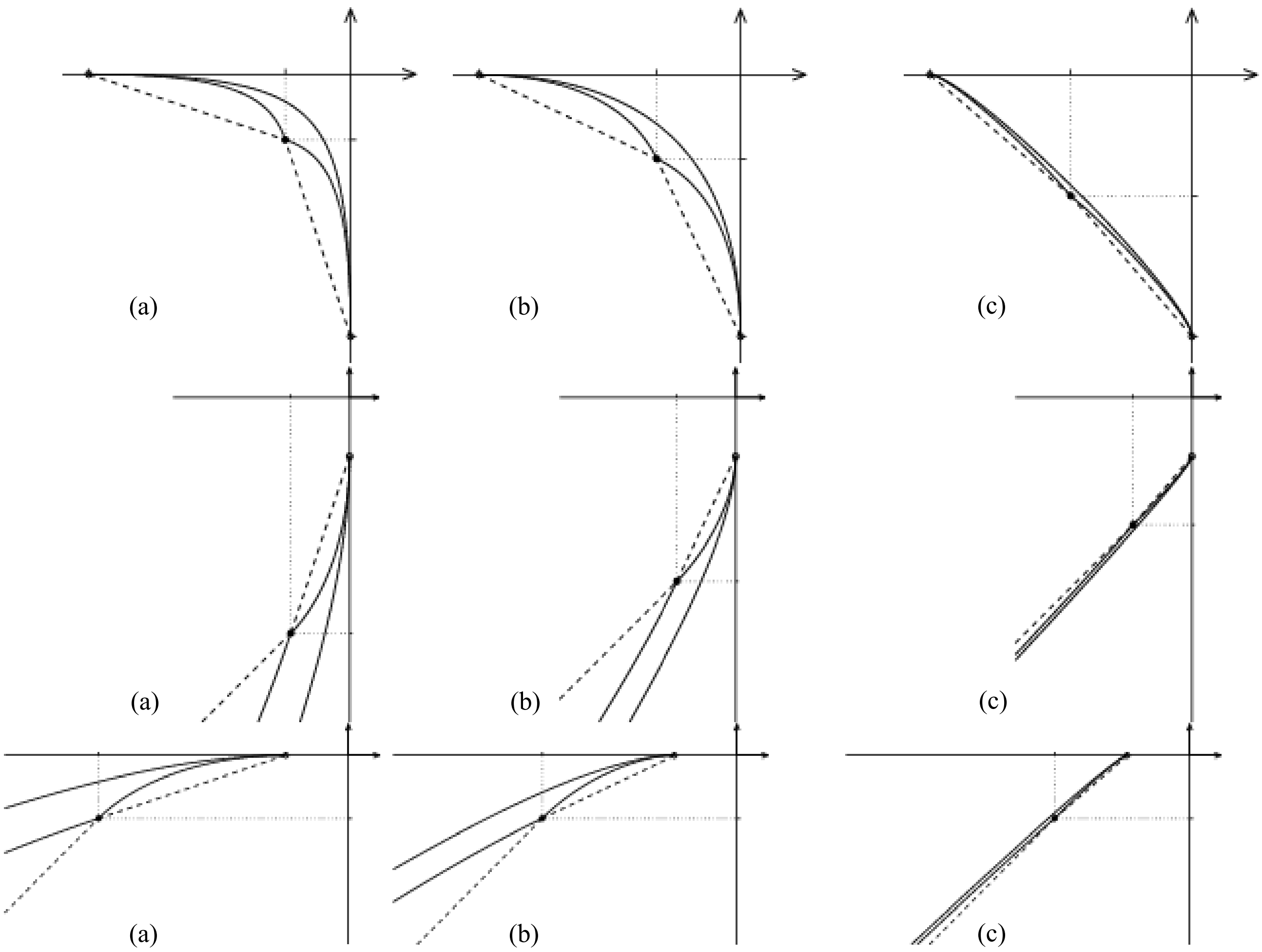

Figure 4: The influence on the shape diagrams by shape parameter α. (a) $\alpha=\dfrac{\pi}{24}$, (b) $\alpha=\dfrac{2\pi}{3}$, (c) $\alpha=\dfrac{23\pi}{24}$.

In case (B) the parametric equations of the curves C, L_i and l_i are determined by:

$$C:\begin{cases} u=\dfrac{2\cos\alpha-\cos(\alpha t)-\cos(\alpha-\alpha t)}{1-\cos(\alpha-\alpha t)}, \\ v=\dfrac{\cos(\alpha t)-1}{1-\cos(\alpha-\alpha t)}, \end{cases} \quad 0<t<1, \qquad (21)$$

$$L_1:\begin{cases} u=\dfrac{\sin\alpha+\sin(\alpha t)-2\alpha t\cos\alpha-\sin(\alpha-\alpha t)}{\sin\alpha-\alpha t-\sin(\alpha-\alpha t)}, \\ v=\dfrac{\alpha t-\sin(\alpha t)}{\sin\alpha-\alpha t-\sin(\alpha-\alpha t)}, \end{cases} \quad 0<t\le 1, \qquad (22)$$

$$L_2:\begin{cases} u=\dfrac{\sin(\alpha t)+2(\alpha-\alpha t)\cos\alpha-\sin(\alpha-\alpha t)-\sin\alpha}{\alpha-\alpha t-\sin(\alpha-\alpha t)}, \\ v=\dfrac{\alpha t-\sin(\alpha t)-\alpha+\sin\alpha}{\alpha-\alpha t-\sin(\alpha-\alpha t)}, \end{cases} \quad 0\le t<1, \qquad (23)$$

$$l_1:(1+u^*)v+u+1=0, u^*\le u<-1, \qquad (24)$$

$$l_2: v-u+(u^*+1)=0, -\infty<u\le u^*, \qquad (25)$$

where $u^*=-2(\sin\alpha-\alpha\cos\alpha)/(\alpha-\sin\alpha)$.

IV. Effect of Shape Parameter on the Distribution Regions

From the properties of curves C, L_i and l_i, we can deduce that when α tends to zero the limit of shape diagrams approach the distribution of shape conditions for planar uniform cubic B-spline segment. As the value of α increasing, the region D is being enlarged and the regions L, N_0, N_1 and N_2 are diminishing, while the region S is fixed. These changes are shown in Fig. 4.

Note that $-2(\sin\alpha-\alpha\cos\alpha)/(\alpha-\sin\alpha)$ approaches -4 and -2 as α tends to 0 and π respectively, we have the following corollary:

Corollary 1: When there is only a single inflection point on the planar C-B-spline segment $\boldsymbol{r}(t)$, we cannot remove it by altering the shape parameter α. When $\boldsymbol{r}(t)$ is globally convex, it remains global convexity regardless of the changes of shape parameter α.

Corollary 2: The planar C-B-spline segment $\boldsymbol{r}(t)$ either has an inflection point or is globally convex regardless of the changes of shape parameter α, when one of the following three conditions holds:

A: $\boldsymbol{a}_1\times\boldsymbol{a}_3\ne 0$, $(u,v)\in\{(u,v)\,|\,-1-u<v<0,-1<u<0\}$.

B: $\boldsymbol{a}_1\times\boldsymbol{a}_2\ne 0$, $(u,v)\in\{(u,v)\,|\,1+v<u<0,v<-1\}$.

C: $\boldsymbol{a}_2\times\boldsymbol{a}_3\ne 0$, $(u,v)\in\{(u,v)\,|\,1+u<v<0,u<-1\}$.

Corollary 3: The planar C-B-spline segment $\boldsymbol{r}(t)$ has either a singularity or two inflection points regardless of the changes of shape parameter α, when one of the following three conditions holds:

A: $\boldsymbol{a}_1\times\boldsymbol{a}_3\ne 0$, $(u,v)\in T_1\cup T_2\cup T_3$,

where

$$T_1=\{(u,v)\,|\,-\frac{1}{4}\le u,v<0\},$$

$$T_2=\{(u,v)\,|\,-\frac{1+v}{4}\le u<-\frac{1}{4},-\frac{1}{4}<v<0\},$$

$$T_3=\{(u,v)\,|\,-\frac{1+u}{4}\le v<-\frac{1}{4},-\frac{1}{4}<u<0\}.$$

B: $\boldsymbol{a}_1\times\boldsymbol{a}_2\ne 0$, $(u,v)\in T_1\cup T_2\cup T_3$,

where

$$T_1=\{(u,v)\,|\,-1\le u<0,v\le -4\},$$

$$T_2=\{(u,v)\,|\,\frac{1+v}{3}<u<-1,v<-4\},$$

$$T_3=\{(u,v)\,|\,-4<v<u-3,-1<u<0\}.$$

C: $\boldsymbol{a}_2\times\boldsymbol{a}_3\ne 0$, $(u,v)\in T_1\cup T_2\cup T_3$,

where

$$T_1=\{(u,v)\,|\,-1\le v<0,u\le -4\},$$

$$T_2=\{(u,v)\,|\,\frac{1+u}{3}<v<-1,u<-4\},$$

$$T_3=\{(u,v)\,|\,-4<u<v-3,-1<v<0\}.$$

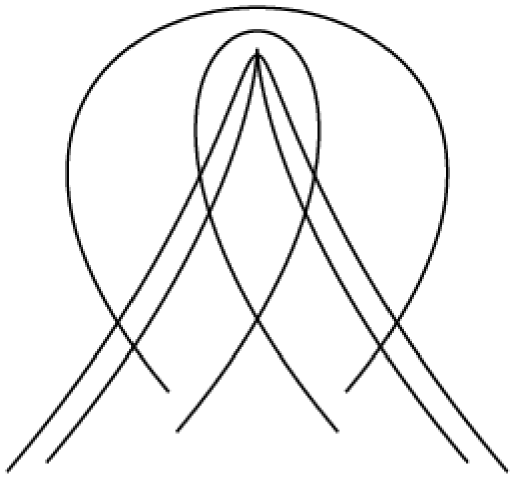

Figure 5: The unwanted shape features is avoided by changing shape parameter.

Corollary 4: If it is possible to change the value of shape parameter α such that the point (u,v) belongs to the region $N_0\cup N_1\cup N_2$, then the unwanted singularities or inflection points of the planar C-B-spline segment $\boldsymbol{r}(t)$ can be avoided (see Fig. 5).

In Fig. 5, $\boldsymbol{d}_0=[0,0]^{\mathrm{T}}\boldsymbol{d}_0=[3,3]^{\mathrm{T}}\boldsymbol{d}_0=[1,3]^{\mathrm{T}}\boldsymbol{d}_0=[4,0]^{\mathrm{T}}$, $(u,v)=(-1/3,-1/3)$; $\alpha=2$, 2.4, 2.6362 and 2.7 correspond to the shape features of global convexity, a loop, a cusp, and two inflection points, respectively.

V. Shape Analysis of Spatial C-B-spline Segments

When $\boldsymbol{d}_i(i=0,1,2,3)$ are not coplanar, the C-B-spline segment $\boldsymbol{r}(t)$ is a spatial curve. Without loss of generality, in this section we suppose that the control points $\boldsymbol{d}_i(i=0,1,2,3)$ are denoted by three dimensional column vectors.

A. The Case of Cusps

If $\boldsymbol{r}(t_0)(0<t_0<1)$ is a cusp of curve (1), then $\boldsymbol{r}'(t_0)=0$. From (1) we have

$$b_0'(t_0)\boldsymbol{a}_1+[b_2'(t_0)+b_3'(t_0)]\boldsymbol{a}_2+b_3'(t_0)\boldsymbol{a}_3=0. \tag{26}$$

Since $\boldsymbol{d}_i(i=0,1,2,3)$ are not coplanar, i.e. $\boldsymbol{a}_i(i=1,2,3)$ are linearly independent, so from (26) we have $b_0'(t_0)=0$ and $b_3'(t_0)=0$. But the fact that $b_0'(t_0)=0$ implies $t_0=1$ contradicts that $b_3'(t_0)=0$ implies $t_0=0$.

Hence there is no cusps on $\boldsymbol{r}(t)$.

B. The Case of Generalized Inflection Points

Definition 7: A point where the torsion

$$\tau(t)=\frac{\det\left(\boldsymbol{r}'(t),\boldsymbol{r}''(t),\boldsymbol{r}'''(t)\right)}{\left|\boldsymbol{r}'(t)\times\boldsymbol{r}''(t)\right|^2}$$

of a spatial curve changes sign is called a generalized inflection point (see [18]).

Let $g(t)=\det\left(\boldsymbol{r}'(t),\boldsymbol{r}''(t),\boldsymbol{r}'''(t)\right)$, by Definition 7, $\boldsymbol{r}(t_0)$ is a generalized inflection point if $g(t)$ changes sign at t_0. Using that $\sum_{i=0}^{3}b_i(t)=1$ holds for all $t\in[0,1]$, we have

$$\begin{aligned}
g(t)&=\begin{vmatrix}\sum_{i=0}^{3}\boldsymbol{d}_i b_i'(t) & \sum_{i=0}^{3}\boldsymbol{d}_i b_i''(t) & \sum_{i=0}^{3}\boldsymbol{d}_i b_i'''(t)\end{vmatrix}\\
&=\begin{vmatrix}\sum_{i=0}^{3}b_i(t) & \sum_{i=0}^{3}b_i'(t) & \sum_{i=0}^{3}b_i''(t) & \sum_{i=0}^{3}b_i'''(t)\\ \sum_{i=0}^{3}\boldsymbol{d}_i b_i(t) & \sum_{i=0}^{3}\boldsymbol{d}_i b_i'(t) & \sum_{i=0}^{3}\boldsymbol{d}_i b_i''(t) & \sum_{i=0}^{3}\boldsymbol{d}_i b_i'''(t)\end{vmatrix}\\
&=\left|\begin{bmatrix}1 & 1 & 1 & 1\\ \boldsymbol{d}_0 & \boldsymbol{d}_1 & \boldsymbol{d}_2 & \boldsymbol{d}_3\end{bmatrix}\begin{bmatrix}b_0(t) & b_0'(t) & b_0''(t) & b_0'''(t)\\ b_1(t) & b_1'(t) & b_1''(t) & b_1'''(t)\\ b_2(t) & b_2'(t) & b_2''(t) & b_2'''(t)\\ b_3(t) & b_3'(t) & b_3''(t) & b_3'''(t)\end{bmatrix}\right|\\
&=\begin{vmatrix}1 & 1 & 1 & 1\\ \boldsymbol{d}_0 & \boldsymbol{d}_1 & \boldsymbol{d}_2 & \boldsymbol{d}_3\end{vmatrix}D(t)\\
&=\begin{vmatrix}1 & 0 & 0 & 0\\ \boldsymbol{d}_0 & \boldsymbol{a}_1 & \boldsymbol{a}_2 & \boldsymbol{a}_3\end{vmatrix}D(t)\\
&=(\boldsymbol{a}_1,\boldsymbol{a}_2,\boldsymbol{a}_3)D(t),
\end{aligned}$$

where $(\boldsymbol{a}_1,\boldsymbol{a}_2,\boldsymbol{a}_3)$ is the blended product of vectors $\boldsymbol{a}_1$, $\boldsymbol{a}_2$ and $\boldsymbol{a}_3$, $D(t)$ is the following determinant:

$$D(t)=\begin{vmatrix}b_0(t) & b_0'(t) & b_0''(t) & b_0'''(t)\\ b_1(t) & b_1'(t) & b_1''(t) & b_1'''(t)\\ b_2(t) & b_2'(t) & b_2''(t) & b_2'''(t)\\ b_3(t) & b_3'(t) & b_3''(t) & b_3'''(t)\end{vmatrix}.$$

It can be easily checked that $D'(t)=0$, consequently $D(t)\equiv D(0)$. A direct computation shows that

$$D(0)=\frac{\alpha^3\sin\alpha}{4(1-\cos\alpha)^2}>0$$

holds for $\alpha\in(0,\pi)$. From the linear independence of $\boldsymbol{a}_1$, $\boldsymbol{a}_2$ and $\boldsymbol{a}_3$, we know that $(\boldsymbol{a}_1,\boldsymbol{a}_2,\boldsymbol{a}_3)\neq 0$. Hence $g(t)$ does not change sign for $0<t<1$, and has the same sign as $(\boldsymbol{a}_1,\boldsymbol{a}_2,\boldsymbol{a}_3)$. It follows that the spatial C-B-spline segment $\boldsymbol{r}(t)$ has no generalized inflection points and has the same rotation direction as its control polygon.

C. The Case of Loops

According to Definition 4, $\boldsymbol{r}(t)$ has a loop means that $\boldsymbol{r}(t)$ intersects itself at $t=t_1$ and $t=t_2$ ($0\le t_1<t_2\le 1$). From (3) we have

$$\begin{aligned}&[b_0(t_2)-b_0(t_1)]\boldsymbol{a}_1+[b_2(t_1)+b_3(t_1)-b_2(t_2)-b_3(t_2)]\boldsymbol{a}_2\\ &+[b_3(t_1)-b_3(t_2)]\boldsymbol{a}_3=0.\end{aligned} \tag{27}$$

Since $\boldsymbol{a}_1$, $\boldsymbol{a}_2$ and $\boldsymbol{a}_3$ are linearly independent, from (27) we have $b_0(t_1)=b_0(t_2)$ and $b_3(t_1)=b_3(t_2)$. Obviously, it is in contradiction to the monotonousness of $b_0(t)$ and $b_3(t)$. Hence there is no loops on spatial C-B-spline segment.

Combining the above results we have the following theorem.

Theorem 2**:** Spatial C-B-spline segment has no cusps, loops or generalized inflection points, and has the same rotation direction as its control polygon. It is a twisted curve.

VI. Conclusion

We investigated the convexity and existence of singularities and inflection points of planar C-B-spline segment. Three kinds of shape diagrams were obtained in terms of the linear independence of the three side vectors. Each of shape diagram is composed of regions which indicate the planar C-B-spline segment having one or two inflection points, or a loop, or a cusp, or be locally or globally convex. Its use enables us to place control points and choose a shape parameter such that the resulting curves have not the undesirable features such as singularities and unwanted inflection points. We also proved that the spatial C-B-spline segment has neither singularities nor generalized inflection points.

References

[1] J. Zhang, “C-curves: An Extension of Cubic Curves,” Computer Aided Geometric Design, Vol. 13, No. 3, 1996, pp. 199-217.

[2] J. Zhang, “Two Different Forms of C-B-splines,” Computer Aided Geometric Design, Vol. 14, No. 1, 1997, pp. 31-41.

[3] E. Mainar and M. Peña, “A Basis of C-Bézier Splines with Optimal Properties,” Computer Aided Geometric Design, Vol. 19, No. 4, 2002, pp. 291-295.

[4] D. Manocha, and J. F. Canny, “Detecting Cusps and Inflection Points in Curves,” Computer Aided Geometric Design, Vol. 9, No. 1, 1992, pp. l-24.

[5] I. Juhász, “On the Singularity of A Class of Parametric Curves,” Computer Aided Geometric Design, Vol. 23, No. 2, 2006, pp. 146-156.

[6] C. Wang, "Shape Classification of the Parametric Cubic Curve and Parametric B-spline Cubic Curve," Computer Aided Design, Vol. 13, No. 4, 1981, pp. 199-206.
[7] B. Su, and D. Liu, "An Affine Invariant and Its Application in Computational Geometry," Scientia Sinica (Series A), Vol. 24, No. 3, 1983, pp. 259-267.
[8] M. C. Stone, and T. D. DeRose, "A Geometric Characterization of Parametric Cubic Curves," ACM Transactions on Graphics, Vol. 8, No. 3, 1989, pp. 147-163.
[9] D. S. Meek and D. J. Walton, "Shape Determination of Planar Uniform Cubic B-spline Segments," Computer-Aided Design, Vol. 22, No. 7, 1990, pp. 434-441
[10] D. S. Kim, "Hodograph Approach to Geometric Characterization of Parametric Cubic Curves," Computer Aided Design, Vol. 25, No. 10, 1993, pp. 644-654.
[11] Z. L. Ye, "Shape Classification of Planar B-spline Cubic Curves", ADVANCES IN CAD/CAM, Proceedings of the Sino-German CAD/CAM Conference, Xi'an, P.R. of China, 1987, pp. 188-196.
[12] Y. Li and R. J. Cripps, "Identification of Inflection Points and Cusps on Rational Curves," Computer Aided Geometric Design, Vol. 14, No. 5, 1997, pp. 491-497.
[13] M. Sakai, "Inflection Points and Singularities on Planar Rational Cubic Curve Segments," Computer Aided Geometric Design, Vol. 16, No. 3, 1999, pp. 149-156.
[14] J. Monterde, "Singularities of Rational Bézier Curves," Computer Aided Geometric Design, Vol. 18, No. 8, 2001, pp. 805-816.
[15] Q. Yang and G. Wang, "Inflection Points and Singularities on C-curves," Computer Aided Geometric Design, Vol. 21, No. 4, 2004, pp. 207-213.
[16] C. Liu and C.R. Traas, "On Convexity of Planar Curves and Its Application in CAGD," Computer Aided Geometric Design, Vol. 14, No. 7, 1997, pp. 653-669.
[17] X. A. Han, X. L. Huang and Y. C. Ma, "Shape Analysis of Cubic Trigonometric Bézier Curves with A Shape Parameter", Applied Mathematics and Computation, Vol. 217, No. 10, 2010, pp. 2527-2533.
[18] R. J. Wu, Guohua Peng and Weimin Luo "Shape Analysis of a class of B-spline curves with shape parameters," Mathematica Numerica Sinica(in Chinese), vol. 32, No. 4, 2010, pp. 349-360.
[19] S. Yang, "A Trust Region Algorithm Using Curve-Linear Searching Direction for Unconstrained Optimization," Journal of Computers, vol. 7, No. 1, 2012, pp. 258-263.
[20] Lin Li, "Conformal Alpha Shape-based Multi-scale Curvature Estimation from Point Clouds," Journal of Computers, vol. 7, No. 6, 2012, pp. 1460-1466.
[21] Y. Liu, "Involute of Cubic Pythagorean-Hodograph Curve," Journal of Computers, vol. 7, No.12, 2012, pp. 2891-2898.
[22] J. W. Bruce and P. J. Giblin, "Curves and Singularities: A Geometrical Introduction to Singularity Theory," New York , Cambridge University Press, 1993, pp. 73-83.

Rongjun Wu was born in Baishui, Shaanxi Province, China, Dec. 1975. He received his Bachelor's degree in 1999, from Department of Mathematics, Northwest University. And then he received his Master's degree in 2005, from School of Science, Northwestern Polytechnical University. His research interests include computer aided geometric design and numerical analysis.

Guohua Peng, born in 1962, professor, Ph. D. supervisor. His current research interests include computer aided geometric design, computer graphics and digital image processing and analysis.